Food Biophysics (2022) 17:508–522
https://doi.org/10.1007/s11483-022-09737-8

ORIGINAL ARTICLE

Impact of Phenolic Acid Derivatives on β-Lactoglobulin Stabilized Oil-Water-Interfaces

Alina Bock[1,2] · Helena Kieserling[2] · Sascha Rohn[2] · Ulrike Steinhäuser[1] · Stephan Drusch[3]

Received: 24 November 2021 / Accepted: 25 March 2022 / Published online: 11 April 2022

Abstract

The physical stability of protein-based emulsions depends on intra- and intermolecular interactions of the interfacial protein-film. As studied in aqueous systems before, phenolic acid derivatives (PADs) non-covalently or covalently crosslink proteins depending on pH-value and thus, may impact interfacial protein-films. Whether these interactions occur in the same manner at the interface as in water and how they vary the properties of the interfacial protein-film has not been clarified. The present study aimed to investigate the interfacial protein-film viscoelasticity and physical emulsion-stability after non-covalently (pH 6.0) and covalently (pH 9.0) crosslinking depending on PAD-structure. For this purpose, we studied an interfacial β-lactoglobulin film with dilatational rheology after crosslinking with PADs, varying in number of π-electrons and polar substituents. Then, we analyzed the physical emulsion-stability by visual evaluation and particle size distribution. The results indicate that PADs with a high number of π-electrons (rosmarinic acid and chicoric acid) weaken the protein-film due to competing of phenol-protein interactions with protein-protein interactions. This is reflected in a decrease in interfacial elasticity. PADs with an additional polar substituent (verbascoside and cynarine) seem to further weaken the protein film, since the affinity of the PADs to the interface increases, PADs preferentially adsorb and sterically hinder protein-protein interactions. In emulsions at pH 6.0 and thus low electrostatic repulsion, PADs promote bridging-flocculation. Due to higher electrostatic repulsion at pH 9.0, the PADs are sterically hindered to form bridges, even though they are polymeric. Hence, our research enables the control of protein-film viscoelasticity and emulsion-stability depending on the PAD-structure.

Keywords β-lactoglobulin · phenolic acid derivative · dilatational rheology · emulsion stability · covalent · non-covalent

Abbreviations

CA	caffeic acid
PAD	phenolic acid derivative
CHA	chicoric acid
RA	rosmarinic acid
CY	cynarine
VD	verbascoside
LVE	linear viscoelastic regime
β-lg	β-lactoglobulin
NLVE	non-linear viscoelastic regime

✉ Alina Bock
a.bock@tu-berlin.de

[1] Department of Food Technology and Food Analysis, Berliner Hochschule für Technik, Luxemburger Straße 10, 13353 Berlin, Germany

[2] Department of Food Chemistry and Analysis, Technische Universität Berlin, Straße des 17. Juni 135, 10623 Berlin, Germany

[3] Department of Food Technology and Food Material Science, Technische Universität Berlin, Straße des 17. Juni 135, 10623 Berlin, Germany

Introduction

Within a wide range of foods, proteins stabilize two- or multi-phase dispersed food systems such as emulsions. Emulsions are thermodynamically instable systems, with the tendency to cream, to flocculate (droplet-droplet interactions), and to coalesce [1]. Besides well-established physical characteristics such as the density of the phases, molecular characteristics affect the properties of the interfacial protein film and the physical emulsion stability. According to interfacial stabilization models, proteins migrate through the bulk water phase of the emulsion, adsorb at the oil-water interface, unfold and structurally align [2, 3]. In the resulting molecular conformation, many proteins show strong intermolecular interactions. Partial unfolding and subsequent protein-protein interactions result in the formation of

a viscoelastic interfacial protein film. These protein-protein interactions include several non-covalent interactions such as hydrogen bonds, hydrophobic interactions, and ionic bonds. Also, intra- and intermolecular covalent bonds like disulfide bridges are newly formed, for example at oxidative conditions, thermal or mechanical treatment and contribute to the formation of a viscoelastic interfacial protein film [2, 4, 5]. The viscoelasticity of an interfacial protein film is characterized by an elastic part, corresponding with the stored energy and a viscous part, referring to the lost energy during mechanical stress in form of deformation. Hence, according to Murray (2011) and Lucassen-Reynders (1993), the viscoelasticity displays the resilience of the interfacial protein film against mechanical stress. Low viscoelasticity leads to breaking up the interfacial film resulting in coalescence [6, 7]. Furthermore, emulsions are stabilized against aggregation and creaming through steric hindrance and electrostatic repulsion of the droplets based on the occupied space and the net charge of the adsorbed proteins, respectively. Charged proteins at the interface result in electrostatic repulsion and thus increase the stability of the dispersed droplets, whereas the proteins show a low net charge near their isoelectric point, the droplets come closer and tend to flocculate, coalesce or cream [8].

It is possible to influence the interactions within the interfacial film. One variant to modify the interactions of interfacial protein films focuses on non-covalently and covalently crosslinking of the adsorbed proteins [9]. Under reducing conditions, mainly non-covalently crosslinks occur, whereas for covalent crosslinks oxidative conditions have to be created, for example by thermal and enzymatic treatment [10–12]. Both processes for covalent crosslinking are accompanied by unfavorable changes in heat-sensitive food ingredients such as unsaturated fatty acids due to direct heat treatment or thermal enzyme inactivation. Therefore, often non-enzymatic processes with crosslinking agents like aldehydes are used [13]. However, the use of aldehydes such as glutaraldehyde or formaldehyde in food is restricted due to their cytotoxicity [14–17]. Possible alternatives for the mentioned crosslinking agents are molecules with a high protein-binding affinity, e.g., phenolic compounds.

In aqueous solutions, protein-phenolic compound interactions have been studied thoroughly in relation to their structural characteristics and the reaction conditions [18, 19]. Phenolic compounds as phenolic acid derivatives (PAD) contain at least one phenyl ring with different hydrophobic and polar substituents. Moreover, the specific type of protein-phenolic compound interactions essentially depends on the reaction conditions. At acidic conditions, phenolic compounds are protonated and interact preferentially non-covalently via hydrogen bonds and hydrophobic interactions (π-electron bonds) with proteins. More specifically, hydrogen bonds are formed between the hydroxyl groups of the phenolic compound and the carbonyl and amino groups of the protein [20]. In comparison to hydrogen bonds, hydrophobic interactions between the hydrophobic regions of the phenolic compound (e.g., through its benzene structure and aliphatic substituents) and hydrophobic domains of the protein (e.g., tryptophan, phenylalanine, and tyrosine residues) represent weak protein-phenolic compound interactions. Consequently, the number of phenyl rings and the number of conjugated π-electrons impact the strength of hydrophobic π-interactions between phenolic compound and protein. By contrast, alkaline reaction conditions favor covalent interactions since phenolic compounds start to deprotonate and their phenolic structures with two ortho- or para-hydroxyl substituents usually tend to form quinones [21, 22]. Quinones then either polymerize with other phenolic compound structures or react with nucleophiles in the protein (e.g., the thiol group of cysteine and amino group of lysine) [23–25].

Regarding protein- phenolic compound interactions at the oil-water-interface, the same kind of interactions are possible. However, targeted crosslinking at the interface using phenolic compounds has not yet been the subject of research. In this case, the adsorbed proteins are partially unfolded at the interface and thus their structure differs from those of dissolved proteins in aqueous solution. More specifically, while hydrophobic domains are buried inside the globular protein structure in water, they are exposed during the partial unfolding of the protein at the oil-water interface [19, 26, 27]. Consequently, other phenolic compound binding sites of the protein are available for protein- phenolic compound interactions at the interface, compared to those in aqueous solution. Recent literature supposed that a targeted crosslinking reaction within the interfacial protein film could be promoted by phenolic compounds with interfacial activity [28, 29]. Polar substituents contribute to an amphiphilic molecule character of the phenolic compound and increase their affinity to the oil-water interface [30]. However, through an amphiphilic molecule character phenolic compounds interact with the interfacial proteins but also competing processes of the proteins are possible. Both possibilities may have an impact on the viscoelasticity of the interfacial protein film. Moreover, emulsion instability processes might be promoted like described for interfacially active low molecular weight substances [31–34]. To what extent phenolic compound-protein interactions compete with protein-protein interactions within the interfacial protein film, disrupt the interfacial film, or stabilize the interfacial protein film through crosslinking, and influence the physical emulsion stability has not been clarified systematically yet.

The present study aimed to investigate the impact of the phenolic acid derivative (PAD) structure on the viscoelastic properties of interfacial protein films and the physical emulsion stability in dependence of the reaction conditions. Therefore, PADs with a varying number in delocalized

π-electrons and polar substituents (Fig. 1) were used. Mostly non-covalent interactions were induced by weak acidic and mostly covalent interaction by weak alkaline crosslinking conditions.

It was hypothesized that the structure of the PADs and crosslinking conditions influence the interfacial protein film properties and emulsion stability as follows:

- The highly amphiphilic molecule character of PADs with polar substituents like sugars favors their adsorption at the oil-water interface and subsequently the disruption of the interfacial protein film by sterical hindrance. As a result, both the elasticity of the interfacial protein film and the emulsion stability decrease.
- Strong hydrophobic interactions between adsorbed proteins and PADs with a high number of conjugated π-electrons result in a decline of protein-protein interactions and a decrease in interfacial elasticity. Furthermore, strong hydrophobic protein-PADs interactions promote intra-droplet interactions, which in turn favors the flocculation of the dispersed droplets in emulsion.
- At weak acidic conditions, protonated PADs and proteins interact mainly non-covalently and the lack of electrostatic repulsion results in a predominantly elastic protein film with a high number of protein-protein interactions. Moreover, in emulsion the lack of electrostatic repulsion leads to bridging-flocculation through interacting PADs.
- At weak alkaline conditions, polymerized PADs are sterically hindered to co-adsorb at the interface, thus, displacement processes are reduced and the emulsions are stable. The negatively charged proteins at the interface repulse each other, resulting in a low number of intermolecular interactions and therefore a decreased interfacial elasticity.

To reach the aim, whey protein ß-lactogloblin (ß-lg) was used as a model substance since its structure and interfacial behavior in emulsion systems is well characterized [27, 35, 36]. The viscoelastic properties of the crosslinked interfacial protein film were studied by dilatational rheology. The physical stability of crosslinked emulsions were studied by the measurement of the oil droplet size by light microscopic and visual evaluation.

Materials and Methods

Preparation of Phenolic Acid Derivative Solutions

PAD solutions with concentrations of 0.2 wt% were prepared and used for dilatational rheology measurements. For emulsion crosslinking following concentrations were used 0.05, 0.54, and 2.71 mmol/l. The PAD was dissolved in distilled water using an ultrasonic bath for 15 min. The solutions were freshly prepared before the measurements to reduce polymerization reactions. The pH value was set to 6.0 or 9.0 at 22 °C with 0.1 M HCl and 0.1 M NaOH (analytical grade, >99.9%, Carl Roth GmbH, Karlsruhe, Germany). Caffeic acid, chicoric acid, cynarine, and verbascoside were purchased from Cfm Oskar Tropitzsch GmbH (>98%, Marktredwitz, Germany). Rosmarinic acid was purchased from Carl Roth GmbH & Co. KG (>98%, Karlsruhe, Germany).

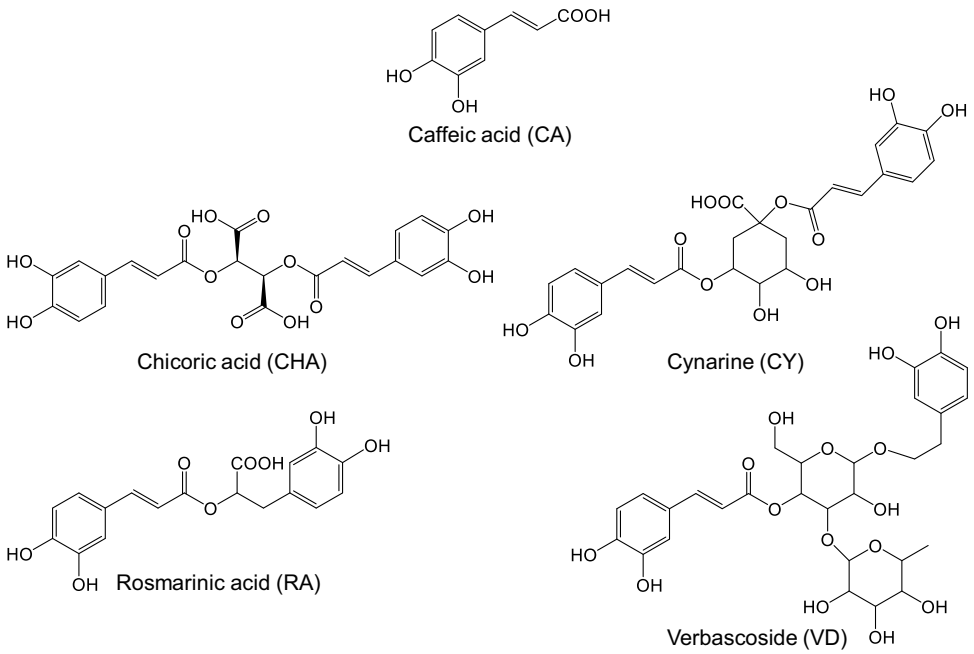

Fig. 1 Structures of the used phenolic acid derivatives (PADs). All PADs are structurally based on caffeic acid (CA) and are interfacially active, except for CA. Chicoric acid (CHA) and cynarine (CY) contain two caffeic acid units, rosmarinic acid (RS) and verbascoside (VD) contain one caffeic acid unit and a substituted dihydroxy-phenol. The CA unit shows a higher number of conjugated π-electrons than the isolated dihydroxy phenyl rings of RS and VD. Consequently, CA units are mesomerically stabilized throughout the molecule. CY and VD are esterified with polar substituents such as quinic acid and rhamnose/glucose.

Preparation of β-Lactoglobulin Solutions

β-lactoglobulin (β-lg) was isolated from whey protein isolate (Davisco Foods International Inc., Le Sueur, Minnesota, USA) as described by Keppler et al. with additional dialysis to remove ions [37]. The purity of 99% was checked with HPLC. For the β-lg solution, β-lg was dissolved in distilled water (6.8 µmol/l, for a 0.1 wt% emulsion), stirred at 22 °C for 60 min, and stored at 8 °C for 16 h. The pH value was set to 6.0 or 9.0 at 22 °C with 0.1 M HCl and 0.1 M NaOH (analytical grade, >99.9%, Carl Roth GmbH, Karlsruhe, Germany). To reduce microbiological spoilage while storage, the solutions were sterile filtered (0.2 µm).

Oil Purification

Linseed oil (cold-pressed organic linseed oil, Biovenue!, Montpellier, France) was used in this study for emulsification to specifically investigate the emulsion properties on a practice-relevant nutritionally valuable unsaturated oil. MCT oil (Medium-chain-triacylglycerols, >99.9%, Witarix MCT 60/40, IOI Oleo GmbH, Hamburg, Germany) was used for dilatational rheology, on the one hand, to allow comparisons with a previous publication and, on the other hand, because it is hardly subject to oxidative changes and thus contributes to reproducible data. To remove interfacially active substances, both oils were purified with Florisil® (MgO × 3.6 SiO2 × 1.53 OH, 100%, Carl Roth GmbH, Karlsruhe, Germany) in a ratio of 3:1 (oil:Florisil®). Therefore, the oil was stirred with a magnetic stirrer for two hours at 22 °C and centrifuged at 10,000 g for 45 min. The purity of the MCT oil was controlled by measuring the interfacial tension against water with a drop tensiometer PAT1-M (Sinterface GmbH, Berlin, Germany). The purified oil showed no decrease in interfacial tension for one hour.

Dilatational Rheology

All interfacial protein films were studied by dilatational rheology with the drop tensiometer PAT1-M (Sinterface GmbH, Berlin, Germany) in a double-needle experiment. The instrument calculates the interfacial tension by fitting the Young-Laplace equation to the droplet profile [32]. In the first step, a droplet with the β-lg solution (see 2.2) (outer needle) with an area of 50 mm^2 was created in MCT-oil. After 20 min of equilibration time, the PAD solution was added through the inner needle by volume exchange. The final PAD concentration in the droplet was 0.1 wt% (PADs are in excess). A camera recorded the droplet profile with one frame per second. After 12 h equilibration time, an amplitude sweep was performed in the range from 1% to 7% deformation amplitude (in 1% steps) as volume-oscillation of the droplet at a frequency of 0.01 Hz. The complex interfacial dilatational modulus (E*) was calculated by the change in the interfacial area (strain) ΔA, which resulted in the change in interfacial tension (stress) ΔIFT. The E* comprises an elastic part E´ (storage modulus) and a viscous part E´´ (loss modulus) [38]. For E´, the linear viscoelastic region (LVE) was defined as 5% deviation of the initial E´. Lissajous-plots (ΔIFT vs. ΔA) were used to depict dilatational behavior in the non-linear viscoelastic (NLVE) region, beyond the LVE [39]. S-factors were calculated to describe the shape of Lissajous-plots for expansion and compression, accordingly [30, 40]. For a system within the LVE, the S-factor tends to zero. Within the NVLE, $S > 0$ indicates strain-stiffening, and $S < 0$ indicates strain-softening of the interfacial film.

Emulsification

Oil-in-water emulsions were prepared at pH 6.0 and 9.0. A coarse emulsion was produced by mixing 80 g β-lg water solution (0.125 wt% β-lg to get 0.1 wt% β-lg within the final emulsion) and 10 g purified linseed oil using a rotor-stator system (Ultra-Turrax T25 basic, IKA -Werke GmbH & CO. KG, Staufen, Germany) at 13,500 rpm for 60 s. The coarse emulsions were homogenized in a high-pressure homogenizer (Panda 2 K, Niro Soavi Deutschland, Lübeck, Germany) at 300 bar with 3 passes. The emulsions were split into 9 g samples and 20 min after emulsification, 1 g of the phenolic acid derivative solutions was added in different concentrations to get a β-lg:PAD molar relations of 1:1, 1:10, and 1:50. The solutions were stirred with a glass rod. An aliquot of the emulsions was transferred into graduated test tubes.

Physical Emulsion Stability

The physical emulsion stability was checked three times within the final storage time of 15 days. An aliquot of the samples was stored at room 20 °C in graduated test tubes and visually evaluated as described in 2.6. Additionally, the oil droplet size was measured by static light scattering (Horiba LA-950, Retsch Technology GmbH, Haan, Germany) to identify instability mechanisms such as coalescence. Therefore, droplets of the samples were diluted in fully desalinated water. The linseed oil refractive index of 1.48 was used for the calculation of the particle size. The results were plotted as a box-whisker plot. The oil droplet size distribution d10 and d90 were depicted as the bottom and the top whisker and the box depicts d25, d50, and d75. The oil droplet size distribution was analyzed by light microscopy (Axiostar plus, Carl Zeiss MicroImaging GmbH, Göttingen, Germany) at 400-fold magnification to differentiate between coalescence and bridging-flocculation.

Statistics

All samples except for dilatational rheology were prepared in triplicates. The samples for dilatational rheology were prepared once with the use of a method standard deviation (n = 6) with 7% for E´ and 28% for E´´.

Results & Discussion

In this study, we crosslink interfacial β-lg films with phenolic acid derivatives (PADs) and determine the protein film viscoelasticity and the physical emulsion stability. For the first time, the structural properties of the phenolic acid derivatives are systematically linked with the resulting interfacial properties of the protein. Thus, in the following two sections we discuss the interfacial film stability against mechanical stress and the physical emulsion stability depending on the PAD structure (varying in the number of delocalized π-electrons and the polar substituents) and the crosslinking conditions (either at weak acidic and weak alkaline conditions).

Interactions with PADs at Weak Acidic Reaction Conditions

PAD-Structure-Dependent Interfacial Protein Film Viscoelasticity Dilatational rheology was used to observe changes in the interfacial protein film viscoelasticity through phenolic crosslinking interactions. The PAD structures vary in the number of conjugated π-electrons (caffeic acid (CA), rosmarinic acid (RA), and chicoric acid (CHA)) and the size of the polar substituent (verbascoside (VD) and cynarine (CY)).

Interfacial protein films are characterized by viscoelastic properties, which are composed of the elastic modulus E` and the viscous modulus E``. For all samples, with and without phenolic crosslinking, E` exceeds E`` at weak acidic conditions at pH 6 (Fig. 2). The β-lg film without phenolic crosslinking shows the highest elasticity of all samples with an elastic modulus E` of approx. 37 mN/m and an LVE until 4% $\Delta A/A_0$. As highlighted by Dickinson (1999), such highly elastic properties of interfacial β-lg films result from strong intermolecular protein-protein interactions, which are based primarily on non-covalent hydrogen bonds, hydrophobic interactions, π-electron bonds, and ionic bonds [41]. Moreover, high interfacial film stability is characterized by pronounced elastic and less pronounced viscous properties [41]. After crosslinking with PADs, the elasticity of the β-lg film decreases over the whole range of oscillation amplitudes depending on the chemical structure of the PAD (Fig. 2). These results are in line with Staszewski et al. (2014), [42] and indicate that protein-PAD interactions compete with the protein-protein interactions at the oil/water interface. For

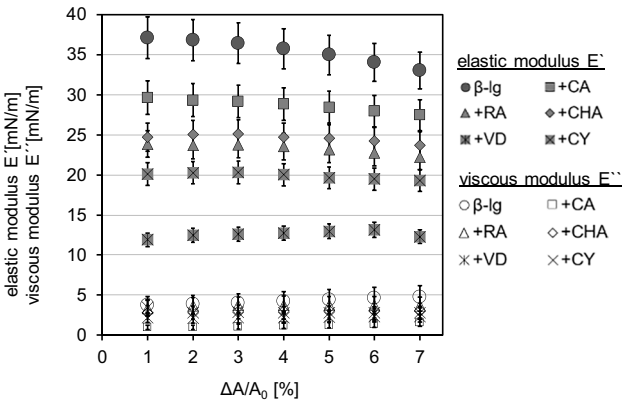

Fig. 2 Viscoelastic properties of the interfacial film at pH 6.0; elastic part E´ and viscous part E´´ for an amplitude sweep between one and 7 % of area oscillation for β-lg with the addition of CA, RA, CHA, VD or CY.

low molecular weight surfactants, it is described that they adsorb in "micro defects" of the interfacial protein film and interact mainly non-covalently for example via hydrophobic interactions or hydrogen bonds with the proteins. Starting from these "micro defects", the proteins get displaced from the interface, and thus intermolecular protein-protein interactions decrease [34, 43]. Comparable to low molecular weight surfactants, we assume that at weak acidic conditions monomeric PADs adsorb in these "micro defects" of the interfacial protein film. This results in competing for intramolecular protein-PAD and intermolecular protein-protein interactions and thus in a decrease of the number of intermolecular interactions, which decreases the elasticity of the interfacial protein film.

PADs like CA (one phenyl ring, small number of π-electrons) result in a minor decrease in initial elasticity (at the strain of 1% $\Delta A/A_0$) to 30 mN/m (Fig. 2). Following Bock et al. (2020), these minor changes can be explained by the low interfacial activity of CA [30], resulting in barely any interactions with the adsorbed β-lg at the oil/water interface. By contrast, PADs like RA and CHA (two phenyl rings, high number of π-electrons) accumulate at the interface due to their amphiphilic structure and lead to a stronger decrease in elasticity than CA to 24 mN/m, and 25 mN/m. Here, the hydrophobic parts of the PAD structure interact with the exposed hydrophobic side chains of the adsorbed β-lg [30, 42]. Thus, it is presumed that mainly the hydrophobic protein-protein interactions compete with hydrophobic protein-PAD interactions. As a result, the number of protein-protein interactions decreases and destabilizes the interfacial protein film, as hypothesized for PADs containing a large π-electron system. A possible explanation is the shift of the amount of intermolecular protein-protein interactions to intramolecular protein-PAD interactions, which may be caused by conformational changes of the proteins through the interactions

described for aqueous systems [44]. Here, the protein may lose its unrestricted unfolded structure at the interface and protein-protein interactions are blocked.

PADs with polar sugar substituents (CY and VD) result in a strong decrease in elasticity, and thus a low protein film viscoelasticity. The lowest initial elasticity is reached by CY with 20 mN/m and by VD with 12 mN/m (Fig. 2). Due to their pronounced amphiphilic character, it was recently postulated that PADs with a polar substituent co-adsorb between the proteins of the interfacial film [30]. Xiao et al. (2011) pointed out that glycosylation of phenolic compounds with sugar moieties weakens protein-PAD interactions through sterical hindrance [45]. Such sterical hindrance may restrict the unfolding through displacement of the adsorbed protein during interfacial film formation. Following the explanation of Benjamins et al. (1996), a minor unfolding of the protein reduces the protein flexibility, the protein-protein interactions, and consequently, the elasticity of the interfacial protein film [42, 46]. Hence, the combination of weak protein-PAD interactions which compete with protein-protein interactions and the sterical hindrance that restricts protein unfolding result in a decrease in intermolecular interactions of the protein film, and thus its elasticity. As hypothesized, the interfacial protein film viscoelasticity is decreasing through interfacial crosslinking with amphiphilic PADs.

The interfacial β-lg film without the addition of PADs shows a short LVE region, (Fig. 2) which is in line with the results of Rühs, Affolter, et al. (2013) [47]. The crosslinking with PADs expands the LVE region of the β-lg film to a range of dilatational strain up to 5% for CA, up to 6% for RA, and up to 7% $\Delta A/A_0$ for CHA, VD, and CY, compared to the β-lg film without crosslinking. In general, the longer the LVE region, the higher the dilatational strain that the interfacial film resists with reversible changes, and hence the higher the number and strength of intermolecular interactions. However, e.g., in the case of low molecular weight surfactants, few intermolecular interactions at the interface result in a long LVE region [47], since fewer interactions can be disrupted through the dilatational strain. Low molecular weight surfactants are characterized by both a low interfacial elasticity over the whole range of dilatational strain and an expanded LVE region [47, 48]. The long LVE region in combination with the low elasticity (Fig. 2), suggest that the interfacial properties of crosslinked β-lg films with PADs approach those of low molecular weight surfactants. Hence, it is assumed that within the LVE region, the crosslinked protein film shows weaker intermolecular interactions than the protein film without crosslinking.

In the NLVE region (beyond LVE), properties of the interfacial film were monitored by the shape of Lissajous-plots (in order to be able to make reliable statements within the NLVE) and the corresponding S-factors. The NLVE region is characterized by irreversible structural changes in the interfacial film through high mechanical stress.

The Lissajous plots at a dilatational strain of 7% $\Delta A/A_0$ are characterized by ellipsoidal shapes including an area (Fig. 3). The ellipse of the β-lg film without phenolic crosslinking shows the largest included area. The phenolic crosslinking results in a decrease of the included area in the following order: RA > CS > VD > CY > CA. This indicates a higher elasticity at high dilatational strain through phenolic crosslinking in comparison to the β-lg film without

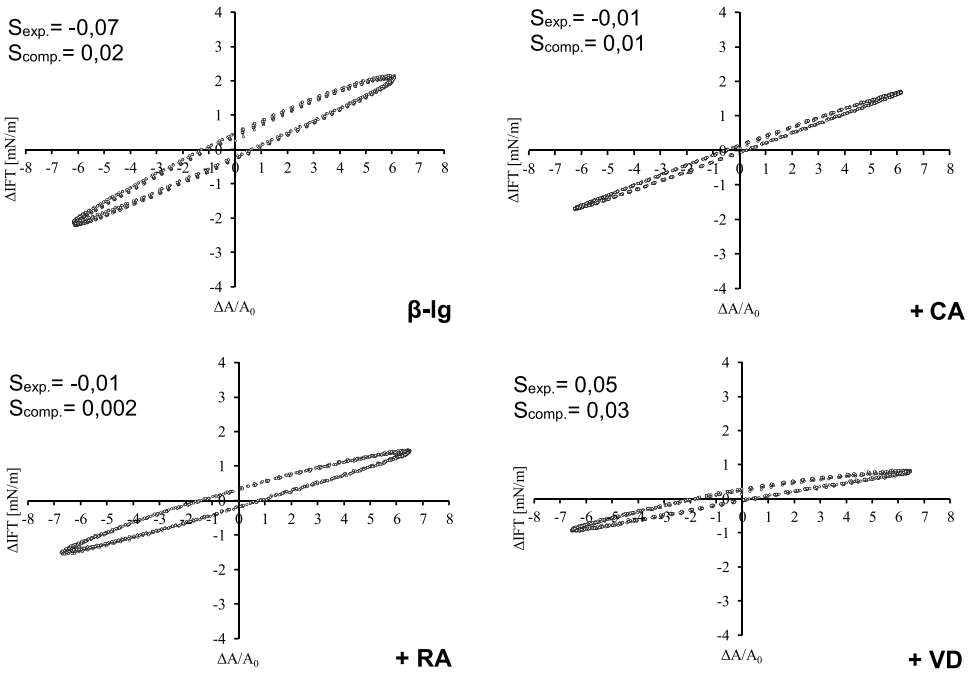

Fig. 3 Lissajous plots as change in interfacial tension against areachange and the belonging S-factors of the dilatational rheology after crosslinking at pH 6.0, the oscillation magnitude of the droplet area is 7% for β-lg and the addition of CA, RA or VD.

crosslinking. Moreover, this result is confirmed by the expanded LVE regions after phenolic crosslinking, and thus less irreversible changes in the interfacial protein network. The calculated S-factor for the β-lg film without phenolic crosslinking is slightly negative for expansion with S = −0,07 (Figs. 3). The S-factors for the β-lg film crosslinked with CA and RA are equal to zero and the s-factor for crosslinking with VD is slightly positive with S = 0,05. However, the differences between all the s-factors identified are considered to be small and not statistically significant, thus they solely indicate a tendency. For compression, the S-factors correspond to values near zero with no differences between all samples. This indicates a low strain stiffening effect due to the phenolic crosslinking during interfacial expansion and linear viscoelastic behavior during interfacial relaxation in case of compression, in which the expanded interfacial area becomes small again. Strain stiffening occurs due to increasing intermolecular interactions resulting in higher stability against deformation through mechanical stress [48]. For low molecular weight surfactants, it is described that they co-adsorb in micro-regions of the interfacial protein film with low protein concentration, described as small "micro defects" of the protein film [34]. The expansion of the interface results in an increasing interfacial area, hence, existing "micro defects" in the interfacial protein film expand and PADs can attach to the interface without competing with interactions between the adsorbed proteins. An expansion-induced interfacial network formation takes place through stronger intermolecular interactions than without expansion. PADs with polar substituents (VD and CY) strengthen the strain stiffening, due to their amphiphilic molecule character, a more targeted attachment in the interfacial "micro defects" and thus a targeted crosslinking in these "micro defects".

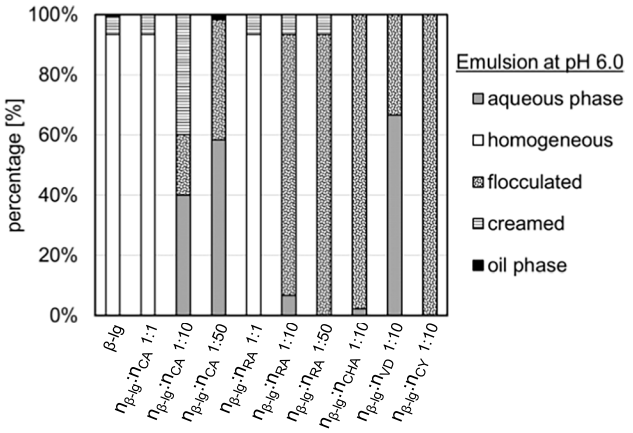

Fig. 4 Visual evaluation of the physical emulsion stability at pH 6.0 after storage depending on molar ratio $n_{β\text{-}lg}:n_{PAD}$. The aqueous phase describes the continuous phase, homogeneous means stable emulsion, flocculated means inhomogeneous emulsion due to flocculation, creamed means a higher oil content than in the homogeneous phase, and oil phase describes free oil on the emulsion surface.

In conclusion, PADs decrease the elasticity of interfacial β-lg films as intramolecular protein-phenol interactions compete with intermolecular protein-protein interactions. A higher number of conjugated π-electrons of the PADs increases the strength of the hydrophobic interactions with the β-lg. Though these higher hydrophobic interactions, intramolecular protein-phenol interactions increases, and further the interfacial elasticity decreases. A further weakening of intermolecular protein interactions is caused by amphiphilic PADs with polar substituents into the LVE, due to adsorption in "micro defects" of the interfacial protein film at the oil-water interface. Due to the spatial expansion of the polar substituents, the protein is additionally hindered in its unfolding. As a result, the intermolecular protein interactions increase. Beyond the LVE the "micro defects" expand, and thus amphiphilic PADs can interact with the interfacial proteins without steric restrictions of the protein folding.

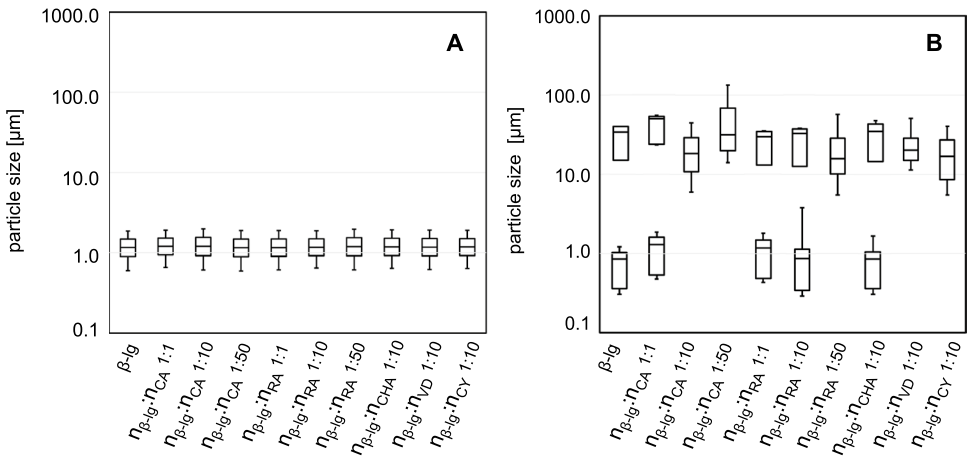

Fig. 5 Particle size distribution of the emulsion at pH 6.0 depending on molar ratio $n_{β\text{-}lg}:n_{PAD}$, the top whisker represents the d90, the upper percentile the d75, the median in the box the d50, the lower percentile the d25, and the bottom whisker the d10, **A**) one hour after PAD-addition, **B**) at the end of storage time.

PAD-Structure-Dependent Physical Emulsion Stability Fig. 6 illustrates the visual physical stability of the emulsions depending on the PAD structure and additionally the molar protein:PAD ratio. Physical emulsion stability can be achieved by electrostatic repulsion of the droplets or the formation of a steric network to protect against coalescence and creaming [49]. At weak acidic conditions (pH 6.0), the β-lg emulsion without crosslinking optically appeared more than 90% as stable homogeneous emulsion, with a minor percentage of creamed (7%) oil droplets after storage time (Fig. 4).

The crosslinking with a PAD with one phenyl ring (CA), and thus one π-electron system for hydrophobic interactions seems to destabilize emulsions, which could be shown in an increased creaming behavior compared to emulsions without crosslinking resulting in 40 – 60% continuous water phase (Fig. 4) and a bimodal particle size distribution (Fig. 5) due to coalescence (Fig. 6) after storage. Precupas et al. (2017) showed that interactions between CA and proteins (here bovine serum albumin) could change the protein conformation [50]. It was suggested that these conformational changes result in decreased electrostatic repulsion, due to the electrostatic shielding of charged amino acids. The lower electrostatic repulsion results in an increased interdroplet interaction between the interfacial proteins themselves or phenolic crosslinks between these proteins, which result in aggregation, creaming, and thus a decreased physical emulsion stability, while intramolecular interactions in the interfacial film are less affected.

The other PADs (RA, CHA, VD, and CY) lead to flocculation and aggregation within the emulsion, without free oil at the top (Fig. 4). The flocculation and aggregation also could be seen in the increasing particle size from 1 µm after preparation up to 50 µm after storage (Fig. 5) and the microscopy (Fig. 6), which confirms the aggregate formation and flocculation. The β-lg emulsion with VD shows the highest instability and strongest flocculation of all samples with approx. 70% of the continuous aqueous phase, and approx. 30% flocculated emulsion (Fig. 4). The addition of CHA and CY seems to result in flocculation without creaming.

Thus, all PADs with two phenyl rings (RA, CHA, VD, and CY) lead to an increased formation of a network between emulsion droplets, resulting in a decreased tendency to coalesce (Fig. 6). The network formation through crosslinking with PADs in protein-gels was described before by Strauss et al. (2004). The authors concluded that the crosslinking results in a higher mechanical strength of the protein gel [23]. Stojadinovic et al. (2013) emphasized that most of the non-covalent interactions between PADs and β-lg depend on their protonation state, and hence on the charge of the compounds [51]. It is reported that proteins have the highest binding capacity for PADs near their isoelectric point because of increasing hydrophobic protein-phenol interactions and a minor electrostatic repulsion [52, 53]. Since the chosen pH is slightly higher than the isoelectric point of β-lg at pH 5.2 [54], both the net charge of the protein within the interfacial film and that of the PADs tend towards zero. Therefore, a strong interfacial protein network can be expected due to barely any electrostatic repulsion and increased hydrophobic interactions [47, 55]. This observation is supported by the dilatation rheology results, which show a high interfacial elasticity, attributed to strong intermolecular interactions within the interfacial protein film (Fig. 2). It is assumed that the presence of at least two phenyl rings and thus a high number of π-electrons in a PAD promotes network

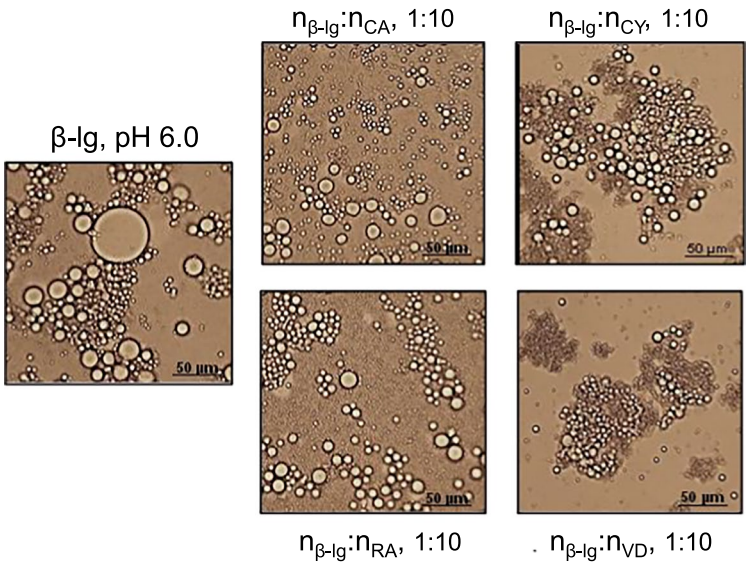

Fig. 6 Microscopy of the emulsion at pH 6.0 after storage with structurally different PADs at the same $n_{β\text{-}lg}:n_{PAD}$ molar ratio of 1:10 at 400fold magnification.

formation due to two hydrophobic protein binding sites. Consequently, the PADs can act as bridging molecules between the interfacial protein films of two droplets. The mechanical strength of the resulting network in turn hinders coalescence [56]. The network seems to be so tight for the PADs with polar substituents (VD and CY) that the network between the droplets is disrupted while storage and the emulsion flocculates (Figs. 5 & 6). Partly this flocculation results in emulsion instability, like in creaming. This increased flocculation might be the result of the competing effects and the steric hindrance through the PADs with polar substituents, as described by the decrease in interfacial elasticity (Fig. 2). PADs with polar substituents disrupt the protein-protein interactions in the interfacial protein film, the interfacial proteins change their conformation, and thus protein-protein interactions between droplets are promoted.

The study also demonstrated that the molar ratio between protein and PAD also has a major impact on emulsion stability. For this purpose, it was assumed that a molar ratio of 1:1 ($n_{\beta\text{-lg}}$:n_{PAD}) not all binding sites on the protein are occupied, at a molar ratio of 1:10 ($n_{\beta\text{-lg}}$:n_{PAD}) most of the binding sites on the protein are estimated to be occupied without an excess of PADs, and at a ratio of 1:50 ($n_{\beta\text{-lg}}$:n_{PAD}) a high proportion of free PADs is present. The addition of PADs in the molecular ratio of 1:1 ($n_{\beta\text{-lg}}$:n_{PAD}) results in an increased emulsion stability since the creamed proportion stays constant but no oil-droplets are broken compared to the β-lg emulsion without crosslinking. $n_{\beta\text{-lg}}$:n_{PAD}-ratios with higher PAD concentration (1:10 and 1:50) result in increasing emulsion instability. Fig. 7 illustrates the microscopic images of the β-lg emulsion with and without the PADs CA and RA with increasing PAD concentration as $n_{\beta\text{-lg}}$:n_{PAD} molar ratio at pH 6.0 after the storage time. The β-lg emulsion without phenolic crosslinking shows inhomogeneous oil droplet sizes from 1 µm to 50 µm. With increasing PAD concentration, the oil droplets decrease to sizes of approx. 1 µm and 20 µm. In the case of the high ratio $n_{\beta\text{-lg}}$:n_{CA} (1:50) with high CA concentration, the oil droplets are broken and a strong aggregation of proteins occurs. In contrast, a molar ratio of $n_{\beta\text{-lg}}$:n_{RA} (1:50) with high RA concentration results in flocculation.

The impact of the PAD concentration is in line with Yang et al. (2015), who described the protein aggregation is depending on the concentration of a phenolic compound. This protein aggregation is explained by a decreased net charge and thus less electrostatic repulsion [57]. Flocculation can be induced by attractive interdroplet interactions like van der Waals, electrostatic, and steric forces, by intermolecular hydrophobic and hydration-repulsion forces between two approaching interfacial films or by molecules acting as bridges between two droplets [1, 58]. Thus, it is presumed that with a higher PAD-concentration combined with low interdroplet repulsion, the more interdroplet crosslinks arise. Interdroplet crosslinks result in flocculation and the physical emulsion stability decreases as hypothesized.

Concluded, for weak acidic crosslinking conditions the emulsion tends to physical instability through flocculation and creaming. It is assumed that the low electrostatic repulsion and the high interaction strength results in decreased emulsion stability. The low electrostatic repulsion enables the droplets to come close to each other, which facilitates the formation of interdroplet-bridges [58]. As a result, PADs can interact with themselves and form bridges between the interfacial films of two approaching droplets. With increasing PAD concentration, PADs in the bulk water phase promote the bridging formation and the emulsion tends to flocculate in the form of bridging-flocculation and subsequently to cream.

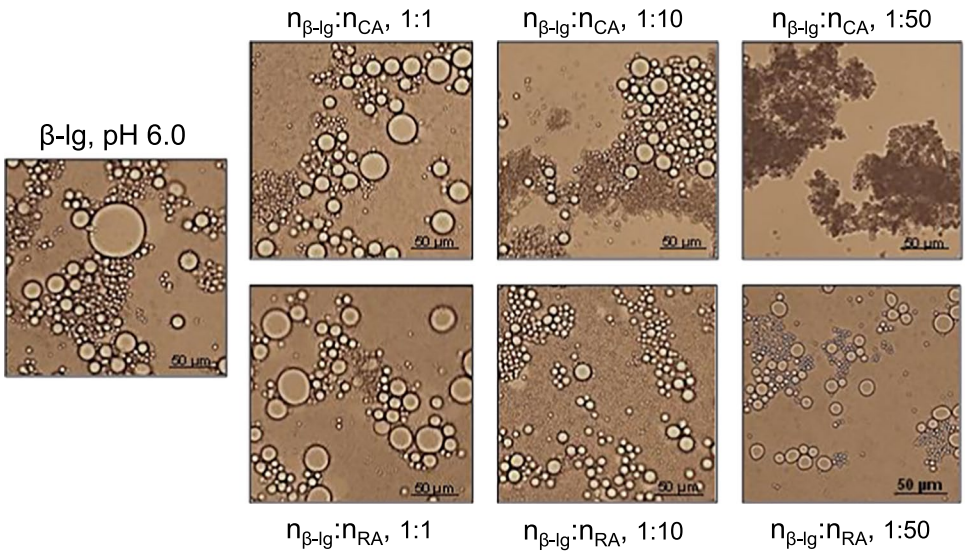

Fig. 7 Microscopy of the emulsion at pH 6.0 after storage with $n_{\beta\text{-lg}}$:n_{PAD} molar ratios with increasing PAD concentration (1:1, 1:10 and 1:50) at 400fold magnification. Caffeic acid represents PADs with one phenyl ring and rosmarinic acid represents PADs with two phenyl rings.

Interactions with PADs at Weak Alkaline Reaction Conditions

Crosslinking-Condition-Dependent Interfacial Protein Film Viscoelasticity

At weak alkaline conditions, with and without phenolic crosslinking, E` exceeds E`` for all samples (Fig. 8). The β-lg film without phenolic crosslinking shows the highest elasticity of all samples with an elastic modulus E` of approx. 33 mN/m and an LVE between 1 and 3% $\Delta A/A_0$ (Fig. 8). The decreased elasticity of the interfacial β-lg film without crosslinking at weak alkaline conditions, in comparison to weak acidic conditions can be explained by the negative net charge of the protein. Stojadinovic et al. (2013) described an partly unfolded molecule structure and deprotonation of amino acid residues above pH 7.5 in aqueous solutions [51]. The negative net charge results in intra- and intermolecular repulsion within the interfacial film, and therefore a low elasticity. After phenolic crosslinking, the decrease in elasticity is less pronounced than at weak acidic conditions.

The crosslinking with PADs results in a reduction of elasticity to 20 – 26 mN/m with minor differences between the samples. The PAD structure seems to have a minor impact on this decrease in elasticity. Since the PADs are partly deprotonated at weak alkaline conditions, they are negatively charged and tend to form quinones and semi-quinones. The quinone formation favors covalent protein-PAD interactions and PAD polymerization [19, 22]. Due to polymerization reactions of the PADs, they change their molecular structure to a higher molecular size [23, 59]. In this context, Strauss et al. (2014) described the dimerization of phenolic acids and the covalently crosslinking with amino acid side chains with amino acids such as lysine and cysteine [23, 24]. Therefore, we assume that polymerization products of

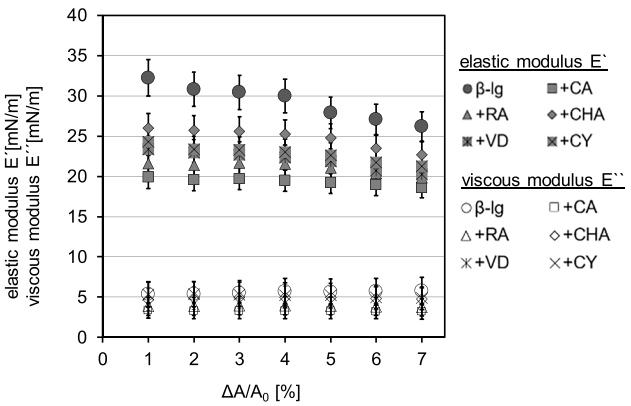

Fig. 8 Viscoelastic properties of the interfacial film at pH 9.0; elastic part E´ and viscous part E´´ for an amplitude sweep between une and 7 % areaoscillation for β-lg with the addition of CA, RA, CHA, VD or CY.

PADs are able to crosslink proteins within the protein film. However, the minor effect of the PADs on the interfacial behavior of the β-lg film might result from reduced possibilities to interact. On the one hand, electrostatic repulsion between PAD and protein is conceivable [53]. On the other hand, the high molecular size of the PADs could prevent their adsorption within the "micro defects" of the interfacial protein film. Thus, as hypothesized, the inter- and intramolecular protein interactions are less displaced than at weak acidic conditions.

The LVE regions of the protein films with phenolic crosslinking are extended at weak alkaline conditions. The LVE regions of the phenolic crosslinked β-lg films at weak alkaline conditions expanded to a range of dilatational strain up to 4% for VD and CY, up to 5% for CHA and RA, and up to 6% $\Delta A/A_0$ for CA, compared to the β-lg film without crosslinking. For all samples, the elastic modulus exceeds the viscous modulus, the latter with values of approx. 5 mN/m.

Beyond the LVE region, the Lissajous plots show increasing viscous properties at alkaline conditions seen in an ellipsoidal shape including a low area (Fig. 9). These increasing viscous properties can be explained by the higher electrostatic repulsion at alkaline conditions, and thus less intermolecular interactions between the interfacial proteins. Strain-softening occurs at weak alkaline conditions. Here the calculated S-factors for all samples are slightly negative for expansion with values between −0.02 and − 0.07 decreasing with phenolic crosslinking. In contrast to the S-factors for expansion, the S-factors for compression are slightly positive for all samples between 0.01 and 0.07. A strain-softening effect was described for the addition of unordered biopolymers (in the form of unordered proteins) to an interfacial protein film, resulting in a softening of interfacial protein films [60]. The softening is explained by the penetration of the interfacial protein film through hydrophobic tails of the biopolymer, which breaks up the integrity of the interfacial protein film by damaging it [60]. Following the given explanation, we assume that at weak alkaline conditions the polymerized PADs behave similar to the described biopolymer and that they come closer to the interface due to the expansion of the "micro defects" in the interfacial film during droplet expansion. The penetration of the interfacial protein film through polymerized PADs results in a steric disturbance of the elastic interfacial film network, and thus in strain-softening.

In summary, the PADs and the β-lg are negatively charged and repulse each other at weak alkaline conditions, resulting in decreased intermolecular interactions compared to weak acidic conditions contrary to the acidic conditions, where the emulsion tends to flocculation due to the lack of electrostatic repulsion. At weak alkaline conditions PADs also tend to quinone formation and polymerization. It is suggested that

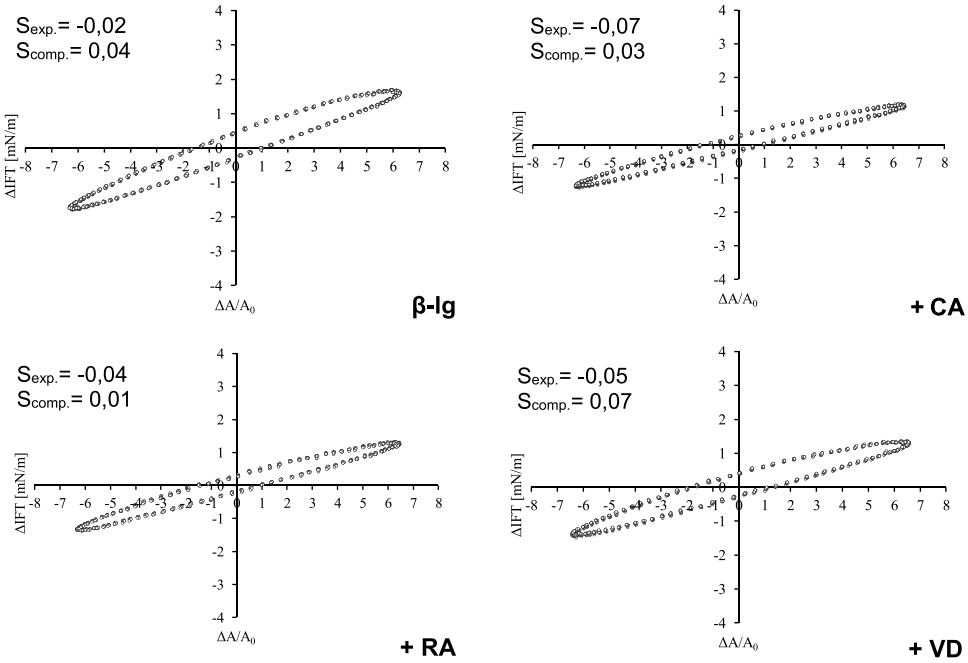

Fig. 9 Lissajous plots as change in interfacial tension against areachange and the belonging S-factors of the dilatational rheology after crosslinking at pH 9.0, the oscillation magnitude of the droplet area is 7% for β-lg and the addition of CA, RA or VD.

the polymerization products are too big contrary to the monomeric PADs at weak acidic conditions to adsorb within the LVE in the "micro defects" of the interfacial film, competing interactions in the interfacial protein film are sterically hindered. Beyond the LVE it is suggested that the "micro defects" in the interfacial film becomes greater, the polymerized PADs can adsorb and strain softening occurs.

Crosslinking-Condition Dependent Physical Emulsion Stability

After storage, the β-lg emulsion at weak alkaline conditions without phenolic crosslinking and those with a molar ratio $n_{β\text{-}lg}$:n_{PAD} of 1:1 are stable and homogeneous (Fig. 10). In comparison to that, the emulsions with a molar ratio of 1:10 ($n_{β\text{-}lg}$:n_{PAD}) with CA and CHA show a similar stability. However, the samples with RA, CY, and VD cream with up to 10%, and additionally, RA and CY form an oil layer on the emulsion surface.

At weak alkaline conditions, the crosslinked emulsions exhibit similar stability with less flocculation and creaming as emulsions without crosslinking (Fig. 10). The particle size distribution (Fig. 11) and the microscopy (Fig. 12) bear out the reduced tendency to flocculate by constant particle size distributions while storage and a homogeneous appearance of the emulsions in the microscopy. Fig. 11 depicts the particle size distribution two hours after PAD-addition and after storage at pH 9.0. Two hours after PAD-addition (to induce the phenolic crosslinking), the emulsions are homogenous with particle sizes of 0.7 µm as the median. After storage, most of the samples show an unchanged monomodal

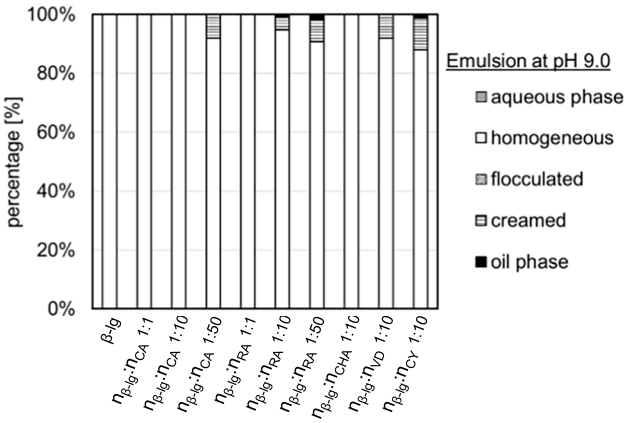

Fig. 10 Visual evaluation of the physical emulsion stability at pH 9.0 after storage depending on molar ratio $n_{β\text{-}lg}$:n_{PAD}. The aqueous phase describes the continuous phase, homogeneous means stable emulsion, flocculated means inhomogeneous emulsion due to flocculation, creamed means a higher oil content than in the homogeneous phase, and oil phase describes free oil on the emulsion surface.

particle size distribution of droplets with 0.7 µm diameter. The particles of phenolic crosslinked emulsions with a higher $n_{β\text{-}lg}$:n_{PAD}-ratio ($n_{β\text{-}lg}$:n_{CA}, 1:50 and $n_{β\text{-}lg}$:$n_{RA,}$ 1:50) and with the PADs, VD and CY ($n_{β\text{-}lg}$:$n_{VD,}$ 1:10 and $n_{β\text{-}lg}$:$n_{CY.}$ 1:10) are scattered more widely or have a bimodal particle size distribution with a median of 0.7 µm and 10 µm, respectively.

Microscopic images of the phenolic crosslinked emulsions with structurally different PADs at the same $n_{β\text{-}lg}$:n_{PAD}-molar ratio of 1:10 at pH 9.0 after storage are depicted in Fig. 12. The emulsions without phenolic

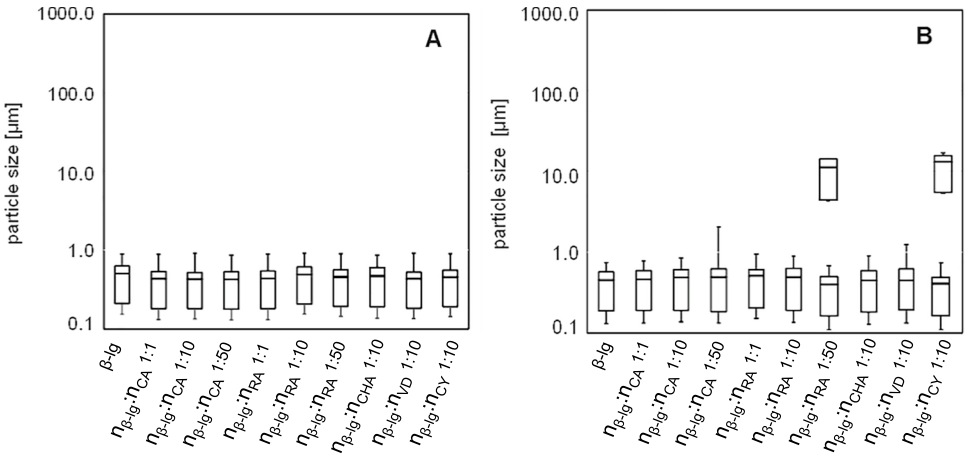

Fig. 11 Particle size distribution of the emulsion at pH 9.0 depending on molar ratio β-lg to PAD, the top whisker represents d90, the upper percentile d75, the median in the box d50, the lower percentile d25, and the bottom whisker d10, **A**) one hour after PAD-addition; **B**) 14 days after PAD-addition.

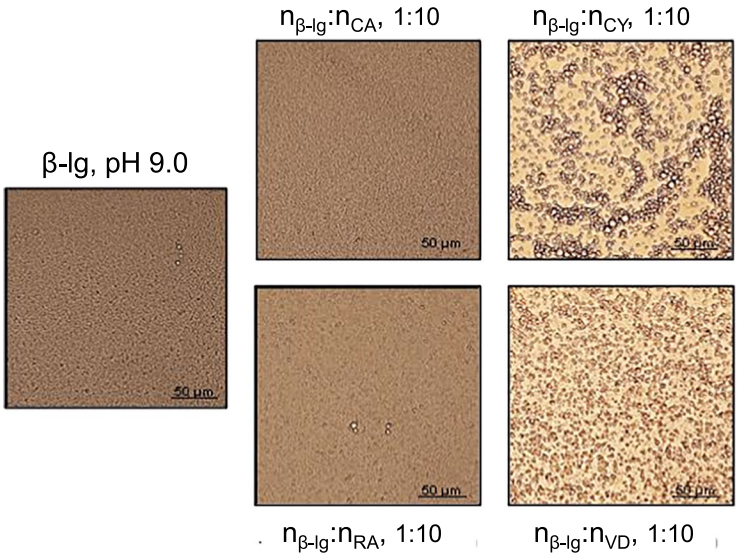

Fig. 12 Microscopy of the emulsion at pH 9.0 after storage with structurally different PADs at the same β-lg:PAD molar ratio of 1:10 molecules at 400fold magnification.

crosslinking and with phenolic crosslinking ($n_{β-lg}:n_{CA}$ and $n_{β-lg}:n_{RA}$, 1:10) show small, homogeneously distributed oil droplets. Furthermore, the addition of the PADs VD and CY (1:10) results in less homogeneous distributed oil droplets, which tend to flocculate.

The higher stability of emulsions at alkaline conditions (Fig. 10) compared to acidic conditions (Fig. 4) can be explained by the increased electrostatic repulsion between the proteins due to increasing protonation. An increased amount of ζ-potential due to the higher charge of β-lg at alkaline conditions was described before [54, 61]. Hence, the oil droplets keep more distance to each other, resulting in a less favored formation of interdroplet bridges through proteins or PADs and a reduced tendency to flocculate, to coalesce, and finally, to cream.

This observation is supported by the dilatation rheology results, which show a reduced interfacial elasticity, attributed to reduced intermolecular interactions within the interfacial protein film (Fig. 8). Also, alkaline quinone formation of the PADs [22], in combination with the increased hydrophobicity of β-lg [61] favors both intramolecular covalent and non-covalent protein-PAD interactions. It is assumed that due to the strong PAD-protein interactions (as well as the polymeric PADs) and the higher droplet repulsion, interdroplet bridging formation is hindered, because the PADs are densely attached to the protein within a droplet. Thus, the small number of interdroplet bridges is resulting in high physical emulsion stability.

Moreover, the emulsion stability was reduced with increasing PAD concentration ($n_{β-lg}:n_{CA}$ and $n_{β-lg}:n_{RA}$, 1:10) with an increased creaming behavior (up to 10%) of the emulsion (Fig. 10). In Fig. 13 the microscopic images of the crosslinked emulsions at pH 9.0 are illustrated for increasing PAD concentration for CA and RA. The β-lg emulsion without phenolic crosslinking shows homogeneous oil droplet sizes (approx. 0.7 µm). For the emulsions with phenolic crosslinking and $n_{β-lg}:n_{PAD}$-molar ratio of 1:50 for RA, the particle sizes of the oil droplets

are scattered widely bearing out the particle size distribution in Fig. 11 and are partly flocculated. For emulsions crosslinked with high concentration of PAD, the microscopy shows a bimodal oil droplet distribution. This indicates that a high number of polymerized PADs enabled a crosslink between the droplets despite the high electrostatic repulsion.

In conclusion, the at weak alkaline conditions mainly covalently crosslinked emulsions, appear mostly homogeneous, due to a high electrostatic repulsion between the proteins. Therefore, the PADs are less prone to form bridges between droplets and thus flocculation. This is in contrast to the emulsion at ph weak acidic conditions, where the electrostatic repulsive forces are low and therefore there is flocculation. Increased bridging-flocculation occurs at increased PAD concentrations at weak acidic and alkaline conditions. This is possible at weak alkaline conditions because a higher number of polymerized PADs is able to bridge even larger distances between droplets.

Conclusion

For the first time, interfacially active phenolic acid derivatives were used for non-covalently and covalently crosslinking of interfacial protein films and systematically linked with the resulting interfacial film properties and emulsion stability. Therefore, the stability of the interfacial film against mechanical stress was studied by dilatational rheology in combination with the physical emulsion stability depending on the phenolic acid derivative structure (varying in the number of delocalized π-electrons and the polar substituents) and the crosslinking conditions (varying between weak acidic for mainly non-covalent and weak alkaline for mainly covalent interactions).

As hypothesized, phenolic acid derivatives decrease the elasticity of interfacial β-lactoglobulin films. Intramolecular protein-phenol interactions compete with intermolecular protein-protein interactions within the interfacial protein film, which result in a decrease in the number of intermolecular interactions. A higher number of conjugated π-electrons of the phenolic acid derivative increases the strength of the hydrophobic protein-phenolic acid derivative interactions, which shifts the interactions to intramolecular protein-phenol interactions and further decreases the interfacial elasticity. Amphiphilic phenolic acid derivatives with polar substituents adsorb in "micro defects" of the interfacial protein film, sterically restrict the unfolding of proteins, which result in weak interactions with proteins and decrease the interfacial elasticity. At weak acidic conditions, the mainly non-covalently crosslinked β-lactoglobulin emulsions show bridging flocculation and creaming. On the one hand, the minor electrostatic repulsion favors intermolecular interactions, and thus the formation of an elastic interfacial protein film. On the other hand, the lack of repulsion promotes crosslinks between droplets as flocculation. The emulsions, which are mainly covalently crosslinked at weak alkaline conditions, appear mostly homogeneous. The phenolic acid derivatives and the proteins are negatively charged and the phenolic acid derivatives tend to quinone formation and polymerization. It is suggested that the polymerization products are too big to adsorb in the "micro defects" of the interfacial film, competing interactions in the interfacial protein film are sterically hindered. Due to the negative charge, the electrostatic repulsion between the proteins increases and

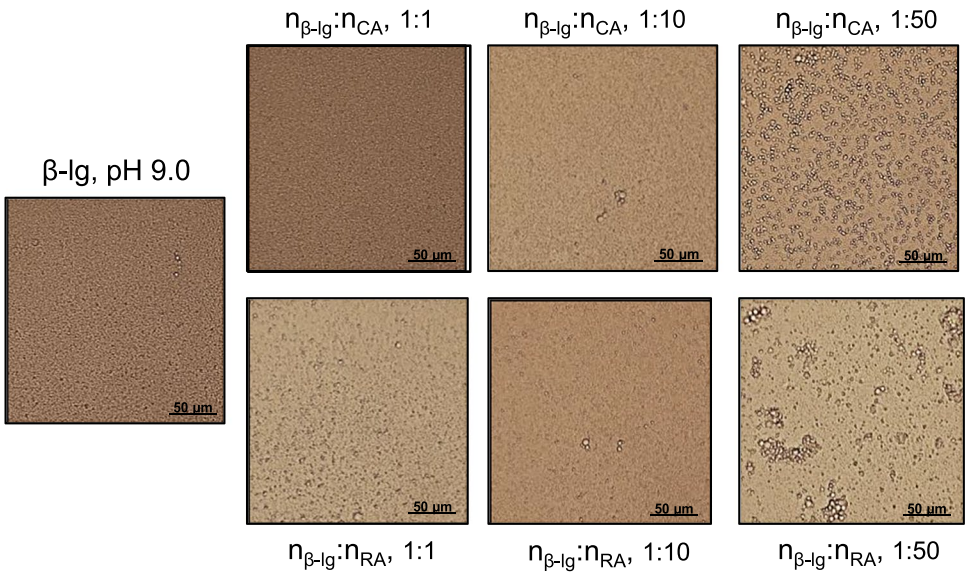

Fig. 13 Microscopy of the emulsion at pH 9.0 after storage with β-lg:PAD molar ratios with increasing PAD concentration (1:1, 1:10 and 1:50) at 400fold magnification. Caffeic acid represents PADs with one phenyl ring and rosmarinic acid represents PADs with two phenyl rings.

the interfacial film is less elastic, as a reduced tendency to emulsion-flocculation develops.

Our results are consistent with the findings of other studies that describes hydrophobic protein-phenol interactions, the weakening of these interactions through polar substituents [62–64]. However, our results extend previous studies through the work at protein stabilized oil-water-interfaces with the use of systematically chosen interfacially active phenolic acid derivatives, which are targeted interacting with the interfacial protein film. To gain more inside into intermolecular interactions between phenolic acid derivatives and interfacial proteins and their impact on emulsion stability, the partitioning behavior of phenolic acid derivatives in protein stabilized oil-water emulsions should be part of future studies. The partitioning behavior should provide information about the portion of interacting phenolic acid derivatives in the interfacial protein film to clarify the impact of the molecule structure on the enrichment in the interfacial protein film, which also indicate different interaction sites at the protein. The partitioning behavior should be studied with chromatographic methods and electron paramagnetic resonance spectroscopy.

Acknowledgement Alina Bock gratefully acknowledges the financial support of the Beuth University of Applied Sciences.

Funding Open Access funding enabled and organized by Projekt DEAL.

Declarations

Conflict of Interest The authors declare that they have no conflicts of interest with respect to the work described in this manuscript.

Ethical Approval Not applicable, because this manuscript does not contain any studies with human or animal subjects.

Informed Consent Not applicable.

References

1. S. Damodaran, Food Sci. **70**, 54 (2005)
2. V. Mitropoulos, A. Mütze, P. Fischer, Adv. Colloid Interface Sci. **206**, 195 (2014)
3. G. Narsimhan, F. Uraizee, Biotechn. Progr. **8**, 187 (1992)
4. E. Dickinson, Food Hydrocoll. **25**, 1966 (2011)
5. S. Damodaran, K. Anand, J. Agric. Food Chem. **45**, 3813 (1997)
6. B.S. Murray, Curr. Opin. Colloid Interface Sci. **16**, 27 (2011)
7. E. Lucassen-Reynders, Food Struct. **12**, 1 (1993)
8. R.S.H. Lam, M.T. Nickerson, Food Chem. **141**, 975 (2013)
9. V.J. Morris, N.C. Woodward, A.P. Gunning, J. Sci. Food Agric. **91**, 2117 (2011)
10. S. Roth, B.S. Murray, E. Dickinson, J. Agric. Food Chem. **48**, 1491 (2000)
11. E. Dickinson, S.T. Hong, J. Agric. Food Chem. **42**, 1602 (1994)
12. D.K. Sarker, P.J. Wilde, D.C. Clark, J. Agric. Food Chem. **43**, 295 (1995)
13. H.M.C. Azeredo, K.W. Waldron, Trends Food Sci. Technol. **52**, 109 (2016)
14. H. He, Y. Wei, H. Luo, X. Li, X. Wang, C. Liang, Y. Chang, H. Yu, Z. Shen, Biotechnol. Prog. **31**, 387 (2015)
15. F.M. Richards, J.R. Knowles, J. Mol. Biol. **37**, 231 (1968)
16. S. Rimdusit, S. Jingjid, S. Damrongsakkul, S. Tiptipakorn, T. Takeichi, Carbohydr. Polym. **72**, 444 (2008)
17. Y.P. Timilsena, B. Wang, R. Adhikari, B. Adhikari, Food Hydrocoll. **69**, 369 (2017)
18. J. Czubinski, K. Dwiecki, Int. J. Food Sci. Technol. **52**, 573 (2017)
19. T. Ozdal, E. Capanoglu, F. Altay, Food Res. Int. **51**, 954 (2013)
20. B. Bartolomé, I. Estrella, M.T. Hernández, J. Food Sci. **65**, 617 (2000)
21. Z. Wei, W. Yang, R. Fan, F. Yuan, Y. Gao, Food Hydrocoll. **45**, 337 (2015)
22. S. Rohn, Food Res. Int. **65**, 13 (2014)
23. G. Strauss, S.M. Gibson, Food Hydrocoll. **18**, 81 (2004)
24. S. Bittner, Amino Acids **30**, 205 (2006)
25. H.M. Rawel, J. Kroll, S. Rohn, Food Chem. **72**, 59 (2001)
26. L. Domínguez-Ramírez, E. Del Moral-Ramírez, P. Cortes-Hernández, M.G. Garibay, J. Jiménez-Guzmán, PLoS One **8**, 1 (2013)
27. J. Zhai, T.J. Wooster, S.V. Hoffmann, T.H. Lee, M.A. Augustin, M.I. Aguilar, Langmuir **27**, 9227 (2011)
28. A.-D. M. Sørensen, A.-M. Haahr, E. M. Becker, L.H. Skibsted, B. Bergenståhl, L. Nilsson, and C. Jacobsen, J. Agric. Food Chem. **56**, 5, 1740–1750 (2008). https://doi.org/10.1021/jf072946z
29. M. Costa, S. Losada-Barreiro, F. Paiva-Martins, C. Bravo-Díaz, Foods **10**, 539 (2021)
30. A. Bock, U. Steinhäuser, S. Drusch, Food Biophys. (2021)
31. F. Tamm, C. Härter, A. Brodkorb, S. Drusch, LWT - Food Sci. Technol. **73**, 524 (2016). https://doi.org/10.1016/j.lwt.2016.06.053
32. S. Böttcher, J.K. Keppler, S. Drusch, Colloids Surfaces A Physicochem. Eng. Asp. **518**, 46 (2017)
33. B. Cai, A. Saito, S. Ikeda, J. Agric. Food Chem. **66**, 704 (2018)
34. A.R. Mackie, A.P. Gunning, P.J. Wilde, V.J. Morris, J. Colloid Interface Sci. **210**, 157 (1999)
35. J.L. Zhai, L. Day, M.I. Aguilar, T.J. Wooster, Curr. Opin. Colloid Interface Sci. **18**, 257 (2013)
36. J. Zhai, A.J. Miles, L.K. Pattenden, T.H. Lee, M.A. Augustin, B.A. Wallace, M.I. Aguilar, T.J. Wooster, Biomacromolecules **11**, 2136 (2010)
37. J.K. Keppler, T. Koudelka, K. Palani, M.C. Stuhldreier, F. Temps, A. Tholey, K. Schwarz, J. Biomol. Struct. Dyn. **32**, 1103 (2014)
38. M. Corzo-Martínez, C. Carrera Sánchez, F.J. Moreno, J.M. Rodríguez Patino, M. Villamiel, Food Hydrocoll. **27**, 438 (2012)
39. P.A. Rühs, N. Scheuble, E.J. Windhab, P. Fischer, Eur. Phys. J. Spec. Top. **222**, 47 (2013)
40. S.E.H.J. Van Kempen, H.A. Schols, E. Van Der Linden, L.M.C. Sagis, Soft Matter **9**, 9579 (2013)
41. E. Dickinson, Colloids Surfaces B Biointerfaces **15**, 161 (1999)

42. M. von Staszewski, V.M. Pizones Ruiz-Henestrosa, A.M.R. Pilosof, Food Hydrocoll. **35**, 505 (2014)
43. B.A. Noskov, M.M. Krycki, Adv. Colloid Interface Sci. **247**, 81 (2017)
44. J. Jia, X. Gao, M. Hao, L. Tang, Food Chem. **228**, 143 (2017)
45. J. Xiao, F. Mao, F. Yang, Y. Zhao, C. Zhang, K. Yamamoto, Mol. Nutr. Food Res. **55**, 1637 (2011)
46. J. Benjamins, A. Cagna, E.H. Lucassen-Reynders, Colloids Surfaces A Physicochem. Eng. Asp. **114**, 245 (1996)
47. P.A. Rühs, C. Affolter, E.J. Windhab, P. Fischer, J. Rheol. (N. Y. N. Y) **57**, 1003 (2013)
48. K. Hyun, M. Wilhelm, C.O. Klein, K.S. Cho, J.G. Nam, K.H. Ahn, S.J. Lee, R.H. Ewoldt, G.H. McKinley, Prog. Polym. Sci. **36**, 1697 (2011)
49. D.J. McClements, Curr. Opin. Colloid Interface Sci. **9**, 305 (2004)
50. A. Precupas, R. Sandu, A.R. Leonties, D.F. Anghel, V.T. Popa, New J. Chem. **41**, 15,003 (2017)
51. M. Stojadinovic, J. Radosavljevic, J. Ognjenovic, J. Vesic, I. Prodic, D. Stanic-Vucinic, T. Cirkovic Velickovic, Food Chem. **136**, 1263 (2013)
52. M. Naczk, S. Grant, R. Zadernowski, E. Barre, Food Chem. **96**, 640 (2006)
53. Q. Zhang, Z. Cheng, Y. Wang, L. Fu, Crit. Rev. Food Sci. Nutr. **0**, 1 (2020)
54. I.J. Haug, H.M. Skar, G.E. Vegarud, T. Langsrud, K.I. Draget, Food Hydrocoll. **23**, 2287 (2009)
55. K. Nagy, M.C. Courtet-Compondu, G. Williamson, S. Rezzi, M. Kussmann, A. Rytz, Food Chem. **132**, 1333 (2012)
56. E. Dickinson, Food Hydrocoll. **68**, 219 (2017)
57. W. Yang, C. Xu, F. Liu, C. Sun, F. Yuan, Y. Gao, J. Agric. Food Chem. **63**, 5046 (2015)
58. E. Dickinson, J. Chem. Soc. Faraday Trans. **88**, 2973 (1992)
59. H. Zhou, B. Zheng, D.J. McClements, J. Agric. Food Chem. (2021)
60. K.D. Danov, P.A. Kralchevsky, G.M. Radulova, E.S. Basheva, S.D. Stoyanov, E.G. Pelan, Adv. Colloid Interface Sci. **222**, 148 (2015)
61. H. Schestkowa, T. Wollborn, A. Westphal, A. Maria Wagemans, U. Fritsching, S. Drusch, J. Colloid Interface Sci. **536**, 300 (2018). https://doi.org/10.1016/j.jcis.2018.10.043
62. C.D. Kanakis, I. Hasni, P. Bourassa, P.A. Tarantilis, M.G. Polissiou, H.A. Tajmir-Riahi, Food Chem. **127**, 1046 (2011)
63. E.H. Liu, L.W. Qi, P. Li, Molecules **15**, 9092 (2010)
64. A.R. Mackie, A.P. Gunning, P.J. Wilde, V.J. Morris, Langmuir **16**, 2242 (2000)